Nb_3Sn Quadrupole Magnets for the LHC IR

G. Sabbi, S. Caspi, L. Chiesa, M. Coccoli, D.R. Dietderich, P. Ferracin, S.A. Gourlay, R.R. Hafalia, A.F. Lietzke, A.D. McInturff, and R.M. Scanlan

Abstract— The development of insertion quadrupoles with 205 T/m gradient and 90 mm bore represents a promising strategy to achieve the ultimate luminosity goal of 2.5×10^{34} $cm^{-2}s^{-1}$ at the Large Hadron Collider (LHC). At present, Nb_3Sn is the only practical conductor which can meet these requirements. Since Nb_3Sn is brittle, and considerably more strain sensitive than NbTi, the design concepts and fabrication techniques developed for NbTi magnets need to be modified appropriately. In addition, IR magnets must provide high field quality and operate reliably under severe radiation loads. The results of conceptual design studies addressing these issues are presented.

***Index Terms*—Interaction Region, Large Hadron Collider, Quadrupole, Superconducting Magnets.**

I. Introduction

HIGH gradient NbTi quadrupoles with 70 mm aperture and operating gradient of 205 T/m are presently being fabricated at FNAL [1] and KEK [2] for the Interaction Regions of the Large Hadron Collider (LHC). These design parameters, which are already at the limit for NbTi magnets, allow for a nominal machine luminosity of 10^{34} $cm^{-2}s^{-1}$. To achieve the ultimate luminosity goal of 2.5×10^{34} $cm^{-2}s^{-1}$, a new generation of IR quadrupoles is required. Several design studies have been performed [3]-[6]: increasing the aperture to 90 mm while maintaining the same field gradient has been identified as the best option. At present, Nb_3Sn is the only superconductor suitable for this application, having demonstrated sufficient performance, availability of wires with adequate piece length, and affordable cost.

The Superconducting Magnet Group at Lawrence Berkeley National Laboratory (LBNL) has extensive experience in the development of Nb_3Sn accelerator magnets, integrating material and cable R&D [7] with the fabrication and test of both shell-type and block-type coils [8] and the development of advanced support structures [9]. The application of these results to the design of second generation LHC IR quadrupoles is discussed, from the viewpoint of magnetic performance (Section II), support structure (Section III) and quench protection (Section III).

Manuscript received August 6, 2001. This work was supported under contract DE-AD03-76SF00098 by the Director, Office of Energy Research, Office of High Energy Physics, U.S. Department of Energy.

All authors are with Lawrence Berkeley National Laboratory, Berkeley, CA 94720 (phone: 001 510 495 2250; fax: 001 510 486 5310; e-mail: glsabbi@lbl.gov).

II. Magnetic Design

A. Superconducting Coils

Both shell ($\cos2\theta$) and block coil geometries can be considered for this application. Shell-type designs generally provide better magnetic efficiency in large aperture magnets. Although superconductor volume is not a key cost issue for the IR quadrupoles, efficient field generation is needed in order to achieve high gradient. The required coil thickness for this application is about 30 mm, which can be obtained using either two or four layers.

A two-layer design of the shell-type requires a Rutherford cable with high aspect ratio and high keystone angle. Such cables lack mechanical stability during winding, and are difficult to fabricate without significant critical current degradation. Previous experience at the LBNL cabling facility indicates that when using conventional techniques, the keystone angle in a two-layer design should be limited to about half of the value needed to maintain radial alignment of the turns (full keystoning). In magnet designs based on partially keystoned cables, wide-angle wedges are needed to restore the Roman arch coil structure, decreasing the magnetic efficiency and causing a mechanical discontinuity. Turns next to such wedges can be critical from the viewpoint of training quenches [10]. In order to overcome these difficulties, we propose a new approach to fabrication of high aspect ratio Rutherford cables. To provide full keystoning while meeting the compaction requirements at both edges, the cables will incorporate special cores made of pure copper, with a central stainless steel foil to avoid eddy currents. The main cable parameters are listed in Table I. A coil cross-section for a two-layer design based on a fully keystoned cable is shown in Fig. 1 (left). The coil is wound as a double layer from a single length of conductor.

TABLE I
Conductor Parameters

Parameter	Unit	2-layer	4-layer	
			Inner	Outer
Strand diameter	mm	0.7	0.8	0.65
Cu/Sc ratio		1.5	1.2	1.6
No. strands		42	17	22
Cable width	mm	15.8	7.7	7.7
Cable mid-thickness	mm	1.45	1.43	1.13
Keystone angle	deg	1.38	1.63	0.89
Insulation thickness	mm	0.1	0.1	0.1
No. turns/octant		36	35	42

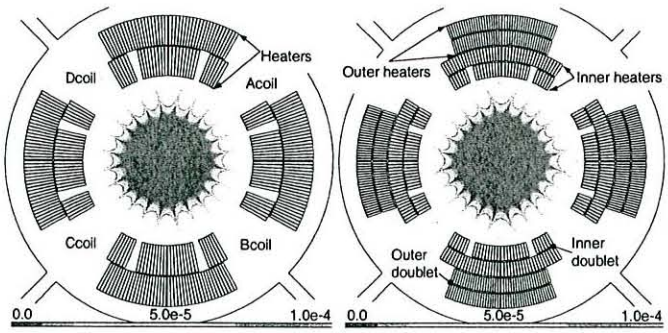

Fig. 1. Coil geometry and field quality at nominal gradient. The innermost contour shows the area with field errors below 0.1 units. Quench heater locations are shown.

A four-layer coil design doubles the fabrication steps with respect to a two-layer design, and results in higher inductance. However, cable requirements for a four-layer design with full keystoning can be met using conventional techniques, and the achievable gradient is significantly higher. The cross-section is shown in Fig.1 (right). The coil consists of two double layers, each wound from a single length of conductor.

Block-type designs have lower magnetic efficiency, but they use high aspect ratio cables with no keystoning. A block design (using either NbTi or Nb_3Sn) was originally proposed for the LHC inner triplet [11]. Experience with Nb_3Sn magnet development has shown that block-type geometries have advantages in terms of conductor compatibility, separation between high field and high stress points, reduction of the peak stress, simplification of support structures and assembly techniques [12]. Preliminary calculations show that the performance parameters for a two-layer block-type coil are comparable to a two-layer shell-type design, with an increase of the conductor area [13]. Further study of block-type coils will be pursued as part of the magnet R&D plan.

B. Magnetic Parameters

The quadrupole short sample limits and operating parameters are given in Table II, assuming 1.9 K operating temperature (T_{op}), and critical current density of 2.4 kA/mm^2 at 12 T, 4.2 K. The four-layer design achieves significantly higher gradient, in particular due to conductor grading and a smaller wedge. At an operational temperature of 4.2 K, the short sample gradient decreases to 229.7 (248.6) T/m in the two-layer (four-layer) design. The four-layer design can still meet the magnet specification at T_{op} = 4.2 K, with a margin of about 20%. No cabling degradation is assumed. This choice is well justified for the four-layer design, which has moderate compaction, aspect ratio and keystone angle requirements. Fabricating a fully keystoned cable for the 2-layer design with no degradation will depend on success of the cable R&D program. The penalty for 10% cabling degradation is rather small, with short sample gradient at T_{op} = 1.9 K of 238.2 (257.5) T/m in the two-layer (four-layer) design.

TABLE II
PERFORMANCE PARAMETERS

Parameter	Symbol	Unit	2-layer	4-layer
Short sample gradient*	G_{ss}	T/m	245.2	265.6
Short sample current*	I_{ss}	kA	17.4	8.7
Coil peak field @Iss	B_{pk}	T	12.6	13.4
Operating current	I_{op}	kA	14.3	6.5
Copper current density @ I_{op}	J_{cu}	kA/mm^2	1.5	1.4
Inductance @ I_{op}	L	mH/m	4.9	23.7
Stored energy @ I_{op}	U	kJ/m	502	508

* J_c(12T, 4.2K)=2.4 kA/mm^2; T_{op}=1.9 K; no cabling degradation assumed.

C. Field Quality

For both designs, the coil geometry has been optimized with ROXIE [14] to achieve geometric harmonics within 0.05 units at a reference radius of 22 mm. The 5 mm increase with respect to the present LHC reference radius of 17 mm is preliminary, and is meant to reflect the larger magnet bore and beam size. It is noteworthy that because of full cable keystoning, the design harmonics do not depend on turn alignment to the inner vs. outer coil radius. This effect caused variations in the calculated harmonics of up to 1 unit (at 17 mm radius) in first generation IR quadrupoles [15].

A cross-section iteration was performed to correct small deviations in b_6 and b_{10} due to iron yoke design and saturation effects. As a result, all design harmonics up to b_{14} are within 0.05 units at the nominal gradient. It is realistic to assume that in order to approach this level of field quality, magnetic measurements of model magnets and correction of the observed systematic values will be required. Magnetic shims located at the magnetic pole, in the gaps between compression pads, will be used for correction of b_6. A similar scheme was successfully demonstrated during the Fermilab LHC IR R&D program [16]. However, magnetic shims were not incorporated in the final design, since the coil fabrication process was shown to ensure adequate field quality. The same assumption cannot be made for Nb_3Sn magnets, due to the difficulty of controlling coil dimensions during the high-temperature reaction phase. A shim thickness of ± 3 mm corresponds to b_6 corrections of ± 0.5 units at nominal gradient. Easy access to the shimming cavity allows one to consider the use of magnetic shims to correct non-allowed low order harmonics after cold magnetic measurements. Both designs feature a single wedge in the inner layer, at the optimal position for correction of systematic deviations of b_{10} with respect to its design value. Changes in the wedge dimension by 150 μm result in a b_{10} correction of 0.05 units. The corresponding change in b_6 is within the tuning capability of the shims.

Iron saturation causes a variation of b_6 in the range of about one unit in the absence of yoke optimization. This drift is probably acceptable since the field quality of the IR magnets is not critical during injection and acceleration. Saturation effects can be reduced to less than 0.1 units over the excitation range using two circular holes at the magnetic mid-plane, with 10 mm and 25 mm radius. These holes can also be used as cooling channels. Other options include shaping the inner surface of the yoke at the magnetic pole, and increasing the size of the gap between compression pads and yoke.

III. Support Structure

The mechanical design of the IR quadrupole (Fig. 2) is based on the use of keys and bladders [17]. This technology has been proven effective on several common coil magnets such as RD3b [9], [18] and RD3c [19] and is implemented here for the first time on a $\cos 2\vartheta$ magnet.

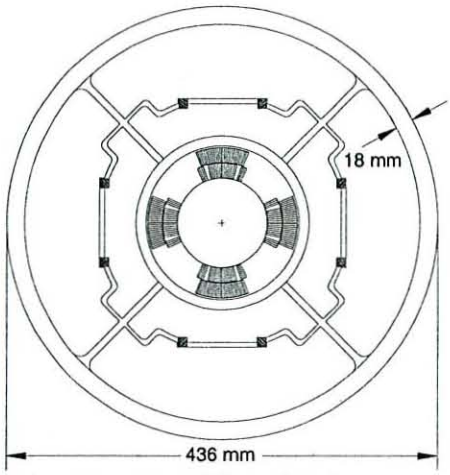

Fig. 2. Proposed support structure of the quadrupole.

The proposed support structure comprises several components: coils, spacers, pads, yokes, and shell. Before the final assembly takes place, the components are assembled into two subassemblies. The first subassembly is composed of two or four layers of conductors and bronze poles, surrounded by adjustable G10 spacers and held together by four bolted iron pads. The pads provide initial pre-stress and alignment. The second subassembly is comprised of a 4-piece iron yoke and an outer aluminum shell. A 5 mm gap is present between pad and yoke. The gap provides room for inserting pressurized bladders and is finally bridged by eight interference keys. The outer diameters of the pad and yoke are 240 mm and 400 mm respectively. The shell is 18 mm thick.

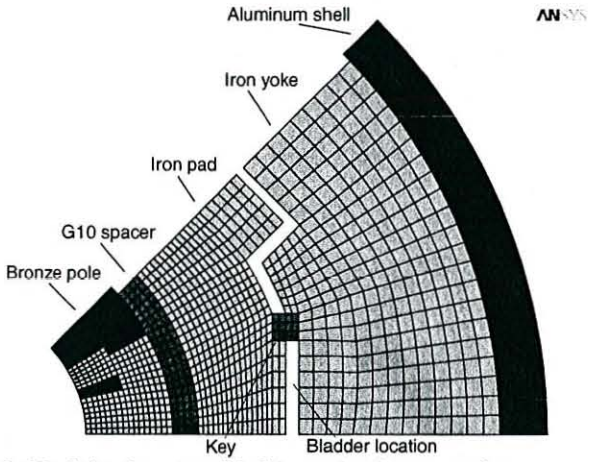

Fig. 3. The finite element model of the quadupole cross-section.

The bladders are made by two stainless steel sheets welded together around their perimeters and pressurized by water. Recent tests showed that they can be pressurized up to about 70 MPa without failure [17]. The bladders provide the force needed to expand the gap between yoke and pad. They simultaneously compress the coil pack and tension the aluminum shell. This process is monitored by strain gauges mounted on the shell: once the desired strain is attained, iron keys can be inserted and the bladders deflated and removed.

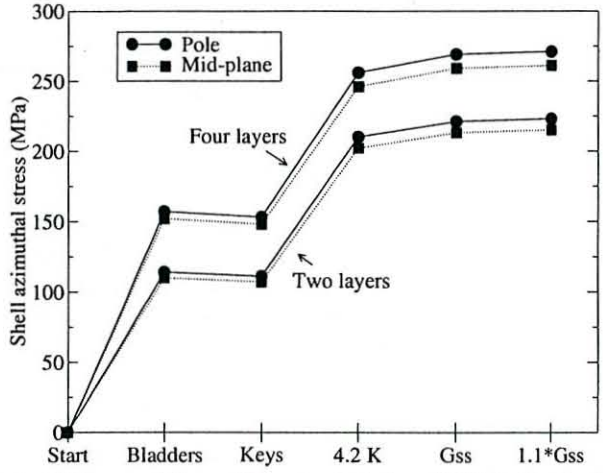

Fig. 4. FEM computations of the azimuthal stress (MPa) in the aluminum shell from assembly to excitation: a safety margin of 10% with respect to the short sample gradient (Gss) has been required as limit condition.

A 2D finite element analysis of the quadrupole (see Fig. 3) has been carried out using ANSYS [20] to simulate bladder pressurization, insertion of interference keys, cool down and magnet excitation. We refer to [21] for the thermo-mechanical properties of the coil. A similar model has been successfully validated by comparing computations and measurements performed on magnet RD3b [17]. In Table III we list calculations of the average pre-stress in the coil (mid-plane and pole region), while the shell stress history is plotted in Fig. 4. Both the two-layer and the four-layer designs have been analyzed. The pressure in the bladders for the two-layer (four-layer) design has been adjusted to 40 MPa (55 MPa) in order to maintain the contact between coil and pole at a gradient of 270 T/m (300 T/m). These limit conditions have been chosen to provide a sufficient safety margin (about 10%) with respect to the short sample conditions.

TABLE III
Azimuthal Pre-stress of the Coil (MPa): Average Values (FEM Computations)

	Inner layer		Outer layer	
	Mid-plane	Pole	Mid-plane	Pole
Two layer design				
Bladders (40 MPa)	62	65	52	59
Keys	62	64	52	56
1.9 K	116	120	100	108
Gradient: 245 T/m	126	30	130	19
Gradient: 270 T/m	130	11	138	4
Four layer design				
Bladders (55 MPa)	85	90	71	81
Keys	86	89	71	77
1.9 K	142	146	121	131
Gradient: 266 T/m	155	41	158	28
Gradient: 300 T/m	162	14	170	5

During the final assembly the azimuthal stress in the shell increases to about 110 MPa (160 MPa) with an interference gap between pad and yoke of 0.45 mm (0.65 mm). The stress remains almost constant after the key insertion. This has been confirmed by measurements on dipole RD3b where a decrease of only 10% in the shell stress occurred after the bladders were deflated.

As already pointed out [17], the azimuthal stress in the shell is expected to double during cool-down due to the difference in thermal contraction between aluminum and iron. Contrary to what is observed in steel collar magnets [22]-[24], with the proposed structure a comparable increase is anticipated for the coil stress.

The results of the numerical calculations show that during excitation the Lorentz forces tend to unload the coil near the pole and gradually increase the stress towards the mid-plane, leaving the stress in the shell unchanged. The coil stress at all stages of assembly and operation is not expected to cause any degradation of the magnet performance [8], [25].

IV. Quench Protection

The proposed designs can be protected with a conventional distributed composite quench heater. The standard designs consist of a 26 μm thick stainless steel heater with distributed Cu (plating or overcoat), sealed in a kapton-heater-kapton laminate. The active length of the heater (stainless steel) is 100 mm, corresponding to 17% of the total heater length. Eleven heaters are used in a 6.5 m long coil. They are located on the outer surfaces of the windings, i.e., for the two-layer design, the bore surface of the inner layer and the outer surface of the outer layer (see Fig. 1). In the four-layer design they are placed on the outer surfaces of the inner and the outer doublets (see Fig. 1).

The 6.5 m version of the two-layer design will require two circuits, each comprising four series circuits: A&B inner layer heaters with C&D outer layer heaters (see Fig. 1) for one circuit and vice-versa for the other. The 6.5 m version of the four-layer design will also require two circuits. The parallel/series circuits feature heaters from both the inner and outer doublets in each series circuit.

Table IV shows the main parameters of the protection system. In the two-layer (four-layer) design a peak coil temperature lower than 200 K (300 K) is expected at the short sample conditions, without a circuit failure and neglecting quench-back effects. The operating condition of both designs (205 T/m) represents a considerable reduction in peak temperature due to the 25% reduction in J_{cu}.

TABLE IV
PROTECTION SYSTEM PARAMETERS

	G_{ss}	Voltage	Capacitance	RC const.	T_{peak}
	T/m	V	mF	ms	K
Two layers	245	440	13.2	26	200
Four layers	266	750	6.2	23	300

V. Conclusions

Design studies of Nb_3Sn quadrupole magnets for second generation LHC IR are described in this paper. Two magnetic designs are presented: a two-layer and a four-layer design. In the two-layer design a special core provides full cable keystoning. The four-layer design reaches a short sample gradient 30% higher than the operational gradient. Nominal harmonics are within 0.05 units at a reference radius of 22 mm. A support structure based on keys and bladders is proposed for the first time for a cos2ϑ magnet. Future plans involve fabrication of a short R&D model using the old LBNL D20 dipole tooling. Winding the coil with dipole-type ends will provide additional cost savings for the R&D model.

References

[1] N. Andreev et al., *IEEE Trans. Appl. Superconduct.*, vol. 11, no. 1, March 2001, pp. 1558-1561.
[2] T. Shintomi et al., *IEEE Trans. Appl. Superconduct.*, vol. 11, no. 1, March 2001, pp. 1562-1565.
[3] S. Caspi et al., Proceedings of the 15th International Conference on Magnet Technology, Beijing, 1997, pp. 175-178.
[4] T. Sen, J. Strait, and A.V. Zlobin, Proceedings of the 2001 Particle Accelerator Conference, Chicago, Illinois, pp. 3421-3423.
[5] J. Strait, Proceedings of the 2001 Particle Accelerator Conference, Chicago, Illinois, pp. 176-180.
[6] A. Zlobin et al., "Large-aperture Nb_3Sn quadrupoles for 2nd generation LHC Interaction Regions", presented at the 8th European Particle Accelerator Conference, Paris, 2002.
[7] R.M Scanlan and D.R. Dietderich, "Progress and plans for the High Energy Physics Conductor Development Program", this conference.
[8] L. Chiesa et al., " Performance comparison of Nb_3Sn magnets at LBNL", this conference.
[9] R.R. Hafalia et al., *IEEE Trans. Appl. Superconduct.*, vol. 12, no. 1, March 2002, pp. 47-50.
[10] N. Andreev et al., *IEEE Trans. Appl. Superconduct.*, vol. 11, no. 1, March 2001, pp. 1637-1640.
[11] W. Scandale and T. Taylor, Proceedings of the 1991 Particle Accelerator Conference, San Francisco, California, pp. 2260-2262.
[12] G. Sabbi, *IEEE Trans. Appl. Superconduct.*, vol. 12, no. 1, March 2002, pp. 236-241.
[13] W. Barletta et al., "LBNL contributions to the US LHC Accelerator Research Program", LBNL-CBP Tech Note 240, March 2002.
[14] S. Russenschuck, Proceedings of the 1st International Roxie Users Meeting and Workshop, Geneva, 1998, p. 1-5.
[15] G. Sabbi et al., Proceedings of the 1997 Particle Accelerator Conference, Vancouver, pp. 3398-3400.
[16] G. Sabbi et al., *IEEE Trans. Appl. Superconduct.*, vol. 10, no. 1, March 2000, pp. 123-126.
[17] S. Caspi et al., *IEEE Trans. Appl. Superconduct.*, vol. 11, no.1, March 2001, pp. 2272-2275.
[18] R. Benjegerdes et al., Proceedings of the 2001 Particle Accelerator Conference, Chicago, Illinois, pp. 208-210.
[19] A.F. Lietzke et al., "Test results for RD3c, a Nb3Sn racetrack dipole magnet", this conference.
[20] ANSYS, licensed by Swanson Analysis Inc., Houston, PA.
[21] K.P. Chow and G.A. Millos, *IEEE Trans. Appl. Superconduct.*, vol. 9, no.2, June 1999, pp. 213-215.
[22] C. Gourdin et al, Proceedings of the 2000 European Particle Accelerator Conference, Vienna, pp. 2136-2138.
[23] A. Devred et al, *IEEE Trans. Appl. Superconduct.*, vol. 11, no. 1, March 2001, pp. 2184-2187.
[24] P. Ferracin et al., *IEEE Trans. Appl. Superconduct.*, vol. 12, no. 1, March 2002, pp. 1705-1708.
[25] D.R. Dietderich, *IEEE Trans. Appl. Superconduct.*, vol. 9, no.2, June 1999, pp. 122-125.